NeuroImage: Clinical 19 (2018) 252–259

Contents lists available at ScienceDirect

NeuroImage: Clinical

journal homepage: www.elsevier.com/locate/ynicl

Longitudinal brain structural alterations in patients with nasopharyngeal carcinoma early after radiotherapy

Zheng Guo[a,c,1], Lujun Han[b,1], Yadi Yang[b], Haoqiang He[b], Jing Li[b], Hong Chen[b], Ting Song[a], Yingwei Qiu[a,*], Xiaofei Lv[b,**]

[a] Department of Radiology, The Third Affiliated Hospital of Guangzhou Medical University, Guangzhou Medical University, Guangzhou, PR China
[b] Department of Medical Imaging, Sun Yat-sen University Cancer Center; State Key Laboratory of Oncology in South China; Collaborative Innovation Center for Cancer Medicine; Guangdong Key Laboratory of Nasopharyngeal Carcinoma Diagnosis and Therapy, Guangzhou, PR China
[c] Department of Oncology, The First Affiliated Hospital of Ganzhou Medical University, Ganzhou, Jiangxi, PR China

ARTICLE INFO

Keywords:
Radiotherapy
Nasopharyngeal carcinoma (NPC)
MRI
Structural
Brain

ABSTRACT

Background and purpose: To investigate effects of radiotherapy on normal brain tissue using in vivo neuroimaging in patients with nasopharyngeal carcinoma (NPC).

Methods and materials: We used longitudinal MRI to monitor structural brain changes during standard radiotherapy in patients newly diagnosed with NPC. We assessed volumetric measures in 63 patients at 2–3 time points before and after radiotherapy, with 20 NPC-free participants as normal controls. Images were processed using validated software (FreeSurfer). Automated results were inspected visually for accuracy. We examined changes in volume of the whole brain, gray matter, white matter, and ventricles, as well as in cerebral volumes partitioned into temporal, frontal, parietal, and occipital lobes. A linear mixed model was used to evaluate longitudinal changes in these measurements. Statistical significance was evaluated at $p < 0.05$, which was corrected for multiple comparisons.

Results: Volumes of the gray matter, and bilateral temporal lobes decreased in a time-dependent manner, whereas ventricle volume showed a time-dependent increase after radiotherapy. No volume changes were detected in NPC patients before radiotherapy when compared normal controls. No volume changes were detected in the subcohort of patients after completion of induction chemotherapy but prior to initiation of radiotherapy. Changes of bilateral temporal lobe volume correlated with irradiation dose in this region. Expansion of the ventricles correlated with a reduction in cognition assessment.

Conclusions: We detected significant and progressive radiotherapy-associated structural changes in the brains of patients with NPC who were treated with standard radiotherapy, especially in the bilateral temporal lobe in which the effect was dose-dependent. Expansion of the ventricles can serve as an imaging marker for treatment-related reduction in cognitive function. Future studies with longer follow-ups are needed to evaluate morphometric changes long-term after radiotherapy.

1. Introduction

Nasopharyngeal carcinoma (NPC) is one of the most common malignant tumors affecting the population in southern China, especially in Guangdong Province (Chan, 2010; Cao et al., 2011). Radiation therapy (RT) with or without adjuvant chemotherapy is the primary treatment modality for patients with NPC (Xu et al., 2017; Wei and Kwong, 2010). The radiation field for NPC encompasses areas adjacent to the primary tumor including the base of skull, which places normal brain tissue, especially the temporal lobe, at risk of injury. After RT, patients often experience cognitive impairment (Hsiao et al., 2010; Kiang et al., 2016; Tang et al., 2012), which may be mediated by injury to the brain, especially regions within the irradiation target. However, brain injury related to irradiation is poorly understood and has no effective prevention or long-term treatment. Current knowledge of irradiation-related brain injury in NPC patients after RT has been derived primarily from studies of animal models or patients with brain tumors (Balentova and Adamkov, 2015; Chapman et al., 2016; Edelstein et al., 2017).

* Correspondence to: Y. Qiu, Department of Radiology, The Third Affiliated Hospital of Guangzhou Medical University, Guangzhou Medical University, Guangzhou, PR China.
** Correspondence to: X. Lv, Department of Medical Imaging, Sun Yat-sen University Cancer Center; State Key Laboratory of Oncology in South China; Collaborative Innovation Center for Cancer Medicine; Guangdong Key Laboratory of Nasopharyngeal Carcinoma Diagnosis and Therapy, Guangzhou, PR China.
E-mail addresses: qiuyw1201@gmail.com (Y. Qiu), lvxf@sysucc.org.cn (X. Lv).
[1] Contribute equally.

https://doi.org/10.1016/j.nicl.2018.04.019
Received 30 January 2018; Received in revised form 29 March 2018; Accepted 16 April 2018
Available online 23 April 2018

However, radiation fields and radiation dosing schemes are quite different between NPC patients and patients with brain tumors or non-central nerve system tumors with prophylactic cranial irradiation. Thus, brain alterations after irradiation may differ between NPC patients and patients with brain tumors. Identification of an accurate and sensitive biomarker of brain injury and neurotoxicity after RT in NPC patients is necessary to develop treatment strategies that may prevent or minimize brain injury.

Ideally, these biomarkers should be obtained during standard treatment planning and follow-up evaluation and correlate with clinical outcome measures of cognitive function. However, to the best our knowledge, no longitudinal studies have explored brain alterations and correlations with irradiation dose or cognitive changes in NPC patients after RT. Our previous cross-sectional studies found that normal-appearing gray matter volume (Lv et al., 2014), bilateral temporal white matter microstructure (Wang et al., 2012) as well as metabolite (Xiong et al., 2013) underwent diverse damaged following RT based on the duration of completion of RT. Moreover, we found that regional gray matter volume loss in the left superior temporal gyrus, left middle temporal gyrus, and right fusiform gyrus negatively correlated with the mean dose to the ipsilateral temporal lobe, which indicated that irradiation-related injury is dose-dependent (Lv et al., 2014). In another cross-sectional study comparing 3 NPC groups with different durations of completion for RT, Wang and colleagues found that gray and white matter mean kurtosis values were significantly higher at 1 week after RT, but significantly lower at 6 months and 1 year after RT; mean diffusivity values were significantly lower at 1 week after RT, but returned to normal by 6 months and 1 year after RT (Wang et al., 2016). These studies suggest that irradiation causes brain injury in NPC patients after RT, and the extent of injury varies depending on the duration of completion of RT. However, cross-sectional studies can be influenced by between-subject variance and possible cohort effects (Schaie, 2005) as well as an inability to detect intra-individual alterations. Thus, a cross-sectional comparison is not sufficient to assess the effects of RT on the brain. Longitudinal studies are needed to elucidate these effects.

In this study, we evaluated longitudinally brain structural alterations related to RT in NPC patients treated with intensity modulated radiotherapy (IMRT) and accounted for potential confounders such as chemotherapy, and age. Based on prior cross-sectional studies in NPC patients after RT (Lv et al., 2014; Wang et al., 2012; Xiong et al., 2013; Wang et al., 2016) and longitudinal studies of patients with brain tumors or non-central nerve system tumors who were treated with prophylactic cranial irradiation (Simo et al., 2016; Prust et al., 2015), we hypothesized the following: (a) Brain structural alterations can accurately detect and monitor RT-induced neurotoxicity in vivo and can be used as a biomarker for noninvasive evaluation of RT-induced brain injury; (b) Longitudinal changes in brain structure, especially in the temporal lobe, are dose dependent; (c) Longitudinal changes in brain structure are time dependent; (d) Longitudinal brain structural changes may underlie cognitive impairment.

2. Materials and methods

2.1. Standard protocol approvals, registrations, and patient consent

Data were obtained through a prospective clinical study of patients with NPC conducted at our institution (ChiCTR-OOB-15006982), which had been registered in the Chinese Clinical Trial Registry (http://www.chictr.org.cn/showproj.aspx?proj=11752). The local institutional review board approved this protocol. All participants provided written informed consent.

2.2. Patients

From December 2014 to November 2017, 83 subjects (with 168 scans) participated in this study. There were 20 NPC-free normal controls (13 male/7 female, 26–58 years old, mean age of 41.0 ± 10.0 years) and 63 patients (43 male/20 female, 21–62 years old, mean age of 39.7 ± 9.3 years) with newly diagnosed, histology-proven, non-keratinizing, undifferentiated NPC. Each patient underwent a detailed pretreatment evaluation, which included a physical examination, nasopharyngeal fiber optic endoscopy, chest radiography, MRI scan of the nasopharynx and brain, abdominal sonography, and whole body bone scan. The clinical stages of NPC were classified according to the American Joint Committee (AJCC) on Cancer staging system (7th edition).

Inclusion criteria for all participants were:

1. Age > 18 years but < 65 years.
2. Baseline Montreal Cognitive Assessment (MoCA) scores equal to or > 26.
3. No intracranial invasion, no distant metastases, no brain tumors, no alcoholism, no substance dependence, no neurological or psychiatric diseases, no prior substantial head trauma, no diabetes, no viral hepatitis, no positive human immunodeficiency virus status, no other major medical illness, not left-handed, and no contraindications for MRI scanning.

For the NPC patients, one more criteria are needed:

4. Must have at least 2 MRI scans: 1 before treatment and 1 at 3 or 6 months after treatment.

Exclusion criteria were:

1. Previous RT of the brain.
2. Contraindications for RT or MR imaging.
3. Other malignant disease that impacted prognosis of the patient and/or was likely to require treatment that would interfere with the study therapy.

2.3. Treatment

All patients were treated with the IMRT technique, which has been described previously (Cao et al., 2011; Xu et al., 2017; Lv et al., 2014; Qiu et al., 2017). Inverse planning was performed on the Corvus System (Peacock; Nomos, Deer Park, IL) using the simultaneous integrated boost technique. Target volumes were delineated slice-by-slice on treatment planning CT scans using an individualized delineation protocol that complies with International Commission on Radiation Units and Measurements reports 62 and 83. The prescribed radiation dose was as follows: a total dose of 68–70 Gy in 30–33 fractions at 2.12–2.33 Gy/fraction to the planning target volume (PTV) of the GTV-P, 60–70 Gy to the nodal gross tumor volume PTV (GTV-N), 60–64 Gy to the PTV of CTV-1 (high-risk regions), and 54–58 Gy to the PTV of CTV-2 (low-risk regions and neck nodal regions). All patients were treated with 1 fraction daily over 5 days per week. The dose-volume statistics for temporal lobes were calculated. Organs at risk were also outlined for dose constraint evaluation. Dose-volume statistics for the temporal lobes are listed in Table 1.

Table 1
Temporal irradiation dose for the 62 NPC patients. Abbreviation: NPC, Nasopharyngeal Carcinoma; N, Number.

Dose information	Dose (Gy)
Temporal.L dose (max)	68.6 (6.6)
Temporal.L dose (min)	2.0 (1.0)
Temporal.L dose (mean)	18.6 (5.8)
Temporal.R dose (max)	69.2 (6.8)
Temporal.R dose (min)	2.0 (1.0)
Temporal.R dose (mean)	18.7 (6.0)

During the study period, institutional guidelines recommended RT alone for stage I, concurrent chemoradiotherapy with/without neoadjuvant adjuvant chemotherapy for stages II to IVA-B. Concurrent chemotherapy was cisplatin weekly or during weeks 1, 4, and 7 of RT. Neoadjuvant therapy consisted of cisplatin with 5-fluorouracil (PF), cisplatin with docetaxel (TP), or cisplatin with 5-fluorouracil and docetaxel (TPF). Neoadjuvant chemotherapy was conducted every 3 weeks for 2 or more cycles. In all, 4 patients were AJCC stage I (6.3%), who received RT only, 59 (93.7%) patients belong to stages II-IV, and all of them received concurrent chemoradiotherapy while 34 of them received neoadjuvant chemotherapy before concurrent chemoradiotherapy.

2.4. MRI acquisition

High-resolution images of the brain were acquired using a T1-weighted 3-dimensional brain volume imaging (3D-BRAVO) sequence with a 3 T GE Discovery MR750 system (GE Medical Systems, Milwaukee, WI). There were 176 contiguous sagittal slices with the following scanning parameters: repetition time (TR) = 8.16 ms, TE = 3.18 ms, inversion time = 800 ms, flip angle = 8°, acquisition matrix = 256 × 256, field of view = 256 × 256 mm^2, isotropic voxel dimensions of 1.0 mm.

2.5. Neurocognitive tests

The MoCA (Beijing Version) was used to assess general cognitive function of NPC patients before and 3 months after treatment. The MoCA assesses different cognitive domains: attention and concentration, executive functions, memory, language, visuoconstruction skills, conceptual thinking, calculations, and orientation. The time to administer the MoCA for each patient was approximately 10 min. The MoCA test has a score range of 0 to 30. All patients with NPC and normal controls completed the MoCA after an appropriate demonstration and explanation on the same day as MRI scanning at baseline, all controls finished MoCA measurements after three months follow-up, while 38 and 27 patients with NPC completed MoCA measurement 3 and 6 months post RT respectively.

2.6. Follow-up procedure

To assess early RT-related brain macrostructural alterations (acute injury and early delayed injury), NPC patients were evaluated at the following time points: before initiation of treatment (baseline), immediately after completion of neoadjuvant chemotherapy treatment (for patients who were treated with neoadjuvant chemotherapy), as well as 3 and 6 months following completion of RT. At each time point, brain structural MRI, nasopharynx and/or neck MRI, as well as neurocognitive tests were performed. Fig. 1 illustrates the procedures for follow-up of patients with NPC.

2.7. Data pre-processing

Automated measurements of brain volumes were standardized across time points and performed using the longitudinal stream in FreeSurfer 5.3.0 (Reuter et al., 2012). Within-subject templates were estimated from images of individual participants in pretreatment and all time points post-treatment. Common information from the template was then used to initialize subsequent processing steps to improve precision and reduce variability. We report brain volumes of total cerebral, gray and white matter, and ventricular areas, as well as cerebral volumes partitioned according to the frontal, parietal, temporal, and occipital lobes. Estimated total intracranial volume (Buckner et al., 2004; Jack Jr et al., 1989) (eTIV) was used as a covariate in all correlational analyses involving brain variables to compensate for inter-individual differences in head size.

3. Statistical analyses

All analyses were performed using open-source R software version 3.0.3 (Team, 2014).

3.1. Statistical analysis of NPC pre-treatment and normal control

Pearson's chi-squared test was used to compare gender differences between the NPC pre-treatment and the normal controls. A two-sample *t*-test was used to compare patient ages across the groups. Univariate analysis was performed to detected MoCA and cerebral differences between groups with age and gender as covariates.

3.2. Statistical analysis of longitudinal changes after RT

We modeled the longitudinal changes in brain macrostructural volume and cognitive performance [without γ_{05} (TIV_j)] using the following linear mixed models (Bates et al., 2014) (Eq. (1)), which modeled fixed and random effects simultaneously, accounting for unequal sampling intervals and missing data (Long, n.d.; Cnaan et al., 1997).

$$Y_{ij} = \gamma_{00} + \gamma_{01}(\text{gender}_j) + \gamma_{02}(\text{education}_j) + \gamma_{03}(\text{age}_j) + \gamma_{04}(\text{TIV}_j) + \gamma_{05}(\text{treatment regimens}_j) + \gamma_{10}(\text{time}_{ij}) + \gamma_{11}(\text{age}_j \times \text{time}_{ij}) + \mu_{0j} + \mu_{1j}(\text{time}_{ij}) + r_{ij} \quad (1)$$

In this equation, Y_{ij} is either brain volumes or MoCA score for the *i*th participant on the *j*th follow-up visit after RT. The longitudinal variable represented the time interval after completion of RT. The pretreatment session with quality structural MRI data and MoCA measurement of each participant was defined as baseline. Time always started from zero. The longitudinal time-dependent effect was expressed as a simple regression between time and Y, plus a residual r.

Gender (male or female) and treatment regimens (with NCT or without NCT) were binary dummy variables, while age and education were the grand-mean-centered versions of the respective variables. Linear mixed model highlights the cross-level interaction effects (Morrell et al., 2009): the intercepts ($\gamma_{00} + \gamma_{01}$ ($gender_j$) + γ_{02} ($education_j$) + γ_{03} (age_j) + γ_{04} (TIV_j) + γ_{05} (treatment $regimens_j$) + μ_{0j}) and the longitudinal changes (γ_{10} ($time_{ij}$) + γ_{11} ($age_j \times time_{ij}$) + μ_{1j} ($time_{ij}$)) were different for each participant (random effect μs), and this difference might be explained by individual differences (fixed effects γs). Specifically, time after completion of RT (time) may proceed at different rates depending on cohort (age) [i.e., γ_{11} ($age_j \times time_{ij}$)].

Using the proposed linear mixed model, we first examined longitudinal time effects (time after completion of RT) on brain macrostructure, followed by MoCA scores. Each of the volumetric measurements and MoCA scores was modeled separately.

To focus on effects of time after completion of RT, we reported longitudinal effects related to time [i.e., γ_{10} and γ_{11} (Eq. (1))]. Statistically significant results at a threshold of $p < 0.05$ passing multiple comparison correction (brain macrostructure: corrected for 12 models) were reported. For cognitive models, we reported time after completion of RT effects with $p < 0.05$.

To determine if induction chemotherapy altered brain macrostructural volume and MoCA results, we ran a paired *t*-test in the subcohort of patients who underwent MRI and MoCA measurements after completion of induction chemotherapy but before initiation of radiotherapy.

3.3. Statistical analyses of associations between cognition and brain irradiation dose

To investigate the associations between alternations of brain structure and cognition in longitudinal trends (Ng et al., 2016), we focused on brain macrostructural volumes that showed significant effects of

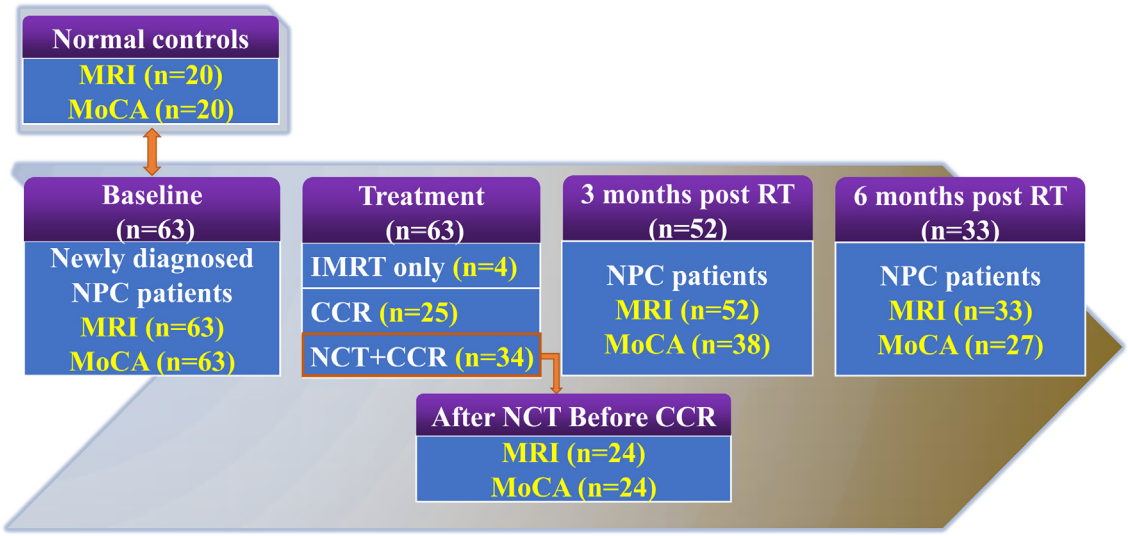

Fig. 1. Flow diagram of participants' enrollment and follow-up.
Abbreviation: NPC, Nasopharyngeal Carcinoma; MoCA, Montreal Cognitive Assessment; RT, Radiotherapy; IMRT, Intensity Modulate Radiotherapy; N, Number; NCT, Neoadjuvant Chemotherapy; CCR, Concurrent Chemotherapy and Radiotherapy.

time after completion of RT (i.e., time or its relevant interactions) and MoCA. We first computed the subject-specific slopes of the regression line between time and the predicted brain macrostructure volumes and MoCA scores. This gave rise to $\beta_{1j.Volume}$ and $\beta_{1j.MoCA}$, respectively. Next, these slopes were evaluated using multiple regression models associating brain macrostructure volumes and MoCA:

$$\beta_{1j.MoCA} = b_0 + b_1(age_j) + b_2(gender_j) + b_3(education_j) + b_4(\beta_{1j.Volume}) + b_5(\beta_{1j.Volume} \times age_j) \quad (2)$$

where b_4 and b_5 are the estimated brain macrostructural volume-MoCA coefficient parameters.

To investigate the associations between alterantions of brain structure and irradiation dose, we also focused on brain macrostructural volumes that showed significant effects of time after completion of RT (i.e., time or its relevant interactions) and irradiation does.

$$\beta_{1j.Volume} = b_0 + b_1(age_j) + b_2(gender_j) + b_3(education_j) + b_4(dose_j) \quad (3)$$

where b_4 is the estimated brain macrostructural volume-irradiation dose coefficient parameter.

4. Results

4.1. Demographic and cognitive measures

The demographic information for the NPC patients and normal controls is shown in Table 2. There were no differences in age, gender, education, MoCA scores (Table 2) and cerebral volume (Supplementary Fig. 1) between NPC pre-treatment and normal controls. The NPC patients had time-dependent lower MoCA scores after RT when compared with baseline (Table 3), however, there were no differences between the baseline and 3 months follow-up in MoCA test for controls ($p = 0.10$).

4.2. Longitudinal changes in brain macrostructural volume

We found significant time-dependent decreases in volumes of the total gray matter, and bilateral temporal lobes as well as significant time-dependent dilation of the ventricles (Fig. 2 and Supplementary Table 1). No significant changes in all measurements of brain volume were observed after induction chemotherapy in the subcohort of NPC patients with induction chemotherapy but before initiation of RT (Supplementary Fig. 2).

Table 2
Demographic characteristics of the NPC patients and normal controls (NCs). Abbreviation: NPC, Nasopharyngeal Carcinoma; Ctrl, Control; MoCA, Montreal Cognitive Assessment; NPC-Pre, patients with Nasopharyngeal carcinoma Pre-treatment; M/F, Male/Female; N, Number.

Demographic information	NCs	NPC-Pre	p values
Numbers	20	63	–
Age (years)	41.0 (10.0)	39.7 (9.3)	0.59
Education (years)	12.0 (3.3)	12.2 (3.2)	0.80
Gender (M/F)	13/7	43/20	0.79
MoCA	28.9 (0.8)	29.0 (1.2)	0.63

Abbreviation: L, Left; R, Right; F, Frontal lobe; T, Temporal lobe; P, Parietal lobe; O, Occipital lobe; V, ventricle; GM, Gray Matter; WM, White Matter; TIV, Total Intracranial Volume.

Table 3
Longitudinal MoCA changes in NPC patients post RT. Abbreviation: NPC, Nasopharyngeal Carcinoma; MoCA, Montreal Cognitive Assessment; RT, Radiotherapy.

Predictor	Coefficient	Standard t error	t	p
Age	−0.03	0.02	−1.67	0.09
Gender	0.25	0.30	0.81	0.41
Education	0.09	0.05	2.03	0.04*
Treatment	−0.33	0.29	−1.12	0.26
Time (post-RT)	−0.28	0.05	−5.55	2.90e-8*
Time * age	0.004	0.006	0.596	0.55

* $p < 0.05$.

4.3. Association between changes in brain macrostructural volume and MoCA scores

Based on longitudinal time effects, 4 brain volume-cognition regressions were conducted, which associated longitudinal changes in MoCA scores with longitudinal changes in total gray matter, bilateral temporal and ventricular volumes. A significant negative correlation was observed between the reduction in MoCA scores and dilation of the ventricles (Fig. 3). Other pairs did not show significant correlations, although trends were observed.

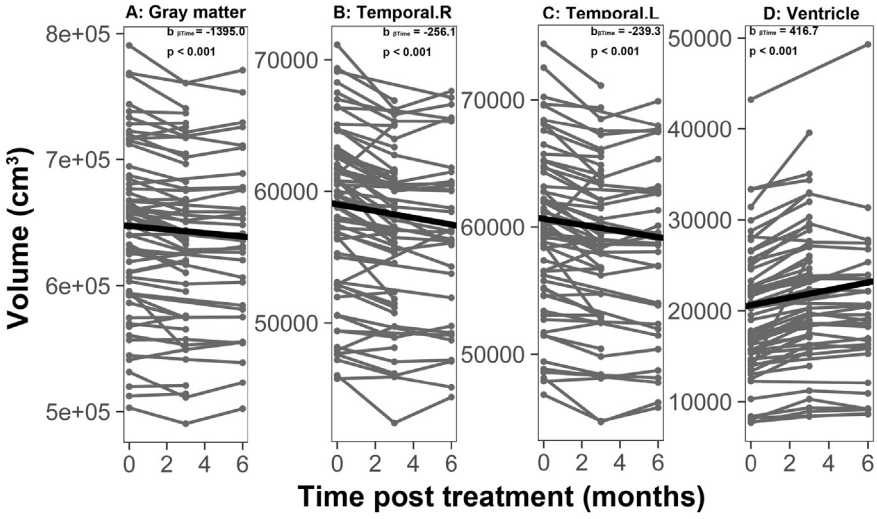

Fig. 2. Time-dependent volumetric alterations in NPC patients after treatment.
Individual trajectories for 4 brain volume measures that showed time-dependent volumetric alterations in NPC patients after treatment. (A) gray matter volume, (B)right temporal volume, (C) left temporal volume and (D) ventricular volume. All volumes are in cm^3.

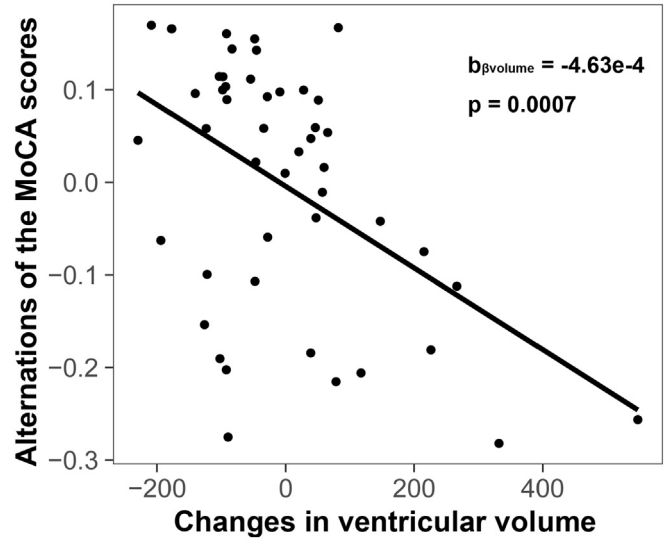

Fig. 3. Expansion of the ventricles correlated with reduction in cognition assessed by MoCA.
Greater dilation of the ventricles was associated with a faster decline in cognition (assessed by MoCA). Each point represents the subject-level longitudinal change in ventricle volume (x-axis, higher values indicate greater dilation of the ventricles) and corresponding longitudinal change in MoCA (y-axis, lower values indicate faster decline in MoCA).

4.4. Association between irradiation dose and changes in brain macrostructural volume

Changes in bilateral temporal lobe volume after RT correlated with irradiation dose of the corresponding temporal lobe (Fig. 4).

5. Discussion

The present longitudinal study tracked brain macrostructural changes in relatively large sample of patients with NPC at 2–3 time points over 6 months after RT. Our results showed time-dependent volumetric decreases for the total gray matter, and the bilateral temporal lobe, as well as time-dependent ventricle expansion in NPC patients after RT. As expected, we also found a dose-dependent effect on the bilateral temporal lobe. Furthermore, longitudinal dilation of the ventricles correlated with the longitudinal reduction of cognition (assessed by MoCA). Moreover, these findings cannot be explained by chemotherapy, given that we did not find any brain or MoCA changes in the subcohort of NPC patients with induction chemotherapy but before initiation of RT. These results demonstrate that use of neuroimaging at multiple time points over several months offers a novel view of the nature, severity, and time course of treatment-associated brain changes in patients with NPC soon after RT, which may underlie cognitive impairment in NPC patients following RT.

We found progressive total gray matter, and bilateral temporal lobe atrophy, as well as time-dependent ventricle expansion in NPC patients after RT, with relative sparing of the parenchymal white matter. Ventricular dilation and cortical atrophy following chemoradiation has been well documented in previous longitudinal CT and MRI studies on chemoradiation for CNS neoplasms (Prust et al., 2015; Stylopoulos et al., 1988; Omuro et al., 2005). Of note, a study (Prust et al., 2015) of patients with glioblastoma who received 6 weeks of chemoradiation followed by up to 6 months of temozolomide chemotherapy alone revealed longitudinal ventricular enlargement accompanied by progressive whole brain and gray matter atrophy while sparing the parenchymal white matter, which is consistent with our present findings. In addition, we also found a significant negative correlation between longitudinal dilation of the ventricles and cognitive impairment. Ventricular dilation has been shown to correlate with gray matter loss (Desikan et al., 2006) and cognitive impairment (Palm et al., 2009) in prior studies. Thus, ventricular dilation may serve as a useful biomarker of cognitive impairment in the clinical setting.

The bilateral temporal lobes showed time-dependent atrophy after RT. These findings are not surprising given that the bilateral temporal lobes are within the irradiation target during RT. In addition, temporal lobe necrosis is the most debilitating late-stage complication after RT in patients with NPC (Chen et al., 2011). The present longitudinal study is consistent to our previous cross-sectional study, by comparing 30 NPC patients with apparently normal-appearing whole brain gray matter after RT and 15 matched controls NPC patients who were newly diagnosed but not yet medically treated. We found that patients who had received RT had gray matter volume decreases mainly in the bilateral temporal lobe, although we did not find time-dependent effects in the cross-sectional study (Lv et al., 2014). Surprisingly, almost all previous cross-sectional studies of irradiation-related brain injury in NPC patients did not find time-dependent effects with diverse modalities such as white matter microstructure (Wang et al., 2012), metabolites (Xiong et al., 2013), and gray matter thickness (Lin et al., 2017). However, consistent with the present study, time-dependent irradiation-related brain injury is well recognized in prior longitudinal studies involving both animal models (Calvo et al., 1988; Gazdzinski et al., 2012; Pellmar et al., 1990) and brain tumor patients (Prust et al., 2015; Connor et al., 2016). Gazdzinski et al. found that widespread developmental deficits

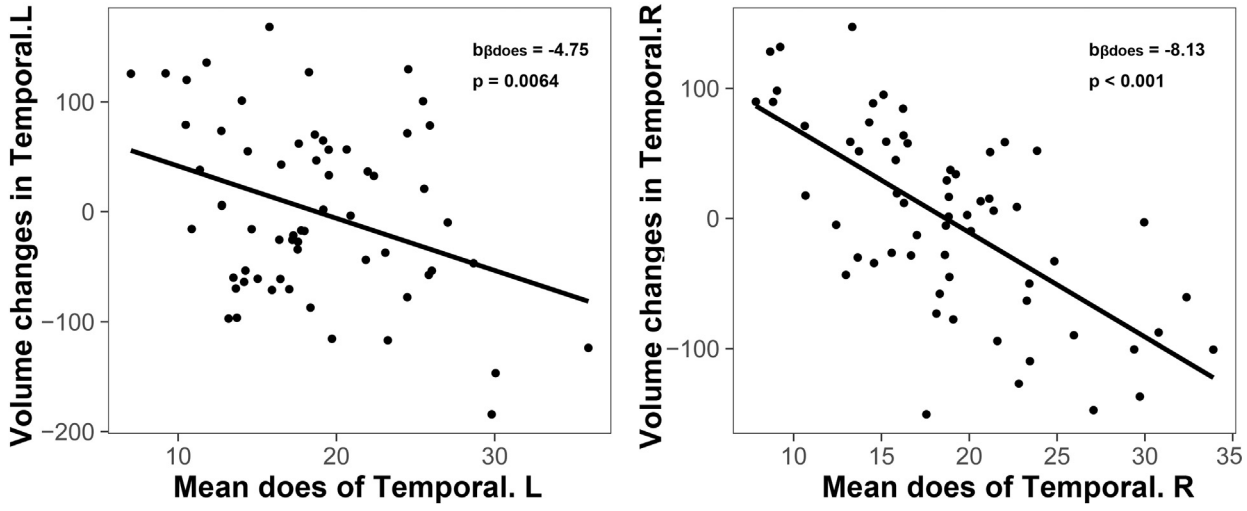

Fig. 4. Does-dependent volume reductions of the bilateral temporal lobe.
Irradiation dose of the temporal lobe correlated longitudinally with temporal atrophy accordingly. Each point represents the subject-level longitudinal volume change of the left/right temporal lobe (y-axis, higher values indicate less atrophy of the left/right temporal lobe) and corresponding irradiation dose (x-axis, lower values indicate less irradiation).

in both white and gray matter persisted or even progressed in a mouse model following whole brain radiation at an infant equivalent age (Gazdzinski et al., 2012). Connor and colleagues used advanced diffusion imaging with different diffusion weightings to show dose-dependent and time-dependent white matter changes, which support a primarily extra-axonal component of white matter injury (Connor et al., 2016). Prust et al. presented evidence of significant, time-dependent, treatment-associated structural brain changes in patients with glioblastoma who were treated with standard chemoradiation (Prust et al., 2015). The discrepancy between cross-sectional and longitudinal studies may be because cross-sectional studies can be influenced by between-subject variance and possible cohort effects (Schaie, 2005). Thus, the present longitudinal findings are more convincing than previous cross-sectional studies, and it is possible for us to demonstrate that irradiation-related brain injury in NPC patients after RT is time-dependent in the early stage (within 6 months). However, our data do not provide conclusive evidence regarding the irreversibility of these changes, as the longest follow-up was 6 months. A lack of evidence showing reversibility within 6 months cannot exclude the possibility that some degree of brain repair leads to partial or complete reversal of morphometric changes in long-term survivors. Exploration of this question awaits further studies assessing patients longitudinally over years rather than months.

Interestingly, we found that the bilateral temporal lobe showed dose-dependent atrophy. Dose-dependent brain injury has been well validated in prior studies (Connor et al., 2016; Petr et al., 2016; Lawrence et al., 2010; Wang et al., 2009). In our previous cross-sectional study, we also found dose-dependent bilateral temporal atrophy (Lv et al., 2014). Irradiation dose-dependent brain atrophy has also been widely documented in previous longitudinal studies of animal models and patients with brain tumors. For example, Karunamuni et al. (2016) found dose-dependent cortical atrophy in high-grade glioma patients after partial brain radiation. Moreover, cortical atrophy was particularly pronounced in the limbic and temporal lobes, which echo the left temporal dose-dependent volume reduction revealed in the current study (Karunamuni et al., 2016). Seibert and colleagues indicated that the hippocampus demonstrates radiation dose-dependent atrophy 1 year after treatment for patients who underwent fractionated, partial brain RT for primary brain tumors when compared with baseline (Seibert et al., 2017). Wang et al. found that a higher radiation dose (30 Gy) induced earlier and more severe histological changes than a lower radiation dose (25 Gy), and these differences were reflected by the magnitude of changes in axial and radial diffusivity (Wang et al., 2009). Petr and colleagues demonstrated that perfusion decreased significantly during the course of radiochemotherapy, and the decrease was higher in regions receiving a higher dose of radiation (Petr et al., 2016). Taken together, the present longitudinal study demonstrates that dose-dependent macrostructural volumetric decreases also occur in NPC patients early after RT, especially in the temporal lobe, which indicates that a safe dose is important for this vulnerable region.

The cellular basis for radiation-associated volumetric reduction in the brain is not well understood. It is believed that at least 3 different types of central nervous system tissue are affected by irradiation: neurons, glia, and blood vessels (Balentova and Adamkov, 2015; Belka et al., 2001). Mature neurons have been considered essentially resistant to therapeutic levels of radiation (Greene-Schloesser et al., 2012; Kim et al., 2014); however, neural progenitor cells within the dentate gyrus and subventricular zone, which are responsible for neurogenesis, are especially radiosensitive and severely depressed in animal models as well as in adult patients after irradiation of malignant brain tumors (Mizumatsu et al., 2003; Monje et al., 2007). In addition to impairing neurogenesis, brain irradiation can kill oligodendrocytes and alter glial turnover (Panagiotakos et al., 2007; Tofilon and Fike, 2000). Moreover, microvascular sequelae of endothelial degeneration, which include telangiectasias, microvascular dilatation, as well as thickening and hyalinization of vessel walls, can occur months to years after the initial radiation-induced injury (Makale et al., 2017; Finet et al., 2010). Such changes can trigger ischemic strokes, cerebral microbleeds, and occlusion of small vessels, leading to local necrosis and extravasation with subsequent demyelination (Desai et al., 2006). Taken together, reductions in neural progenitor cells and oligodendrocytes as well as microvascular sequelae could have led to the macrostructural volumetric reduction and ventricular dilation observed in the present study. However, the precise underlying mechanisms must be elucidated by future studies combining MRI volumetric measurements and histological evaluation.

The present study has several limitations. First, the MoCA is a brief cognitive screening tool that is not sensitive to certain domains, such as executive functions, verbal and visual memory, and attention, which have been shown to be impaired by irradiation in previous studies (Zhang et al., 2015; Greene-Schloesser and Robbins, 2012). Therefore, a comprehensive cognitive evaluation should be performed in a future study. Second, most of all participants enrolled in the present study were treated concurrently with chemotherapy and RT. Although we did

not find any induction chemotherapy-related brain volumetric changes in the subcohort, chemotherapy or synergy between chemotherapy and RT may have affected results in the present study. A future study should enroll chemotherapy only and RT only groups to elucidate such effects. Finally, although our findings provide strong evidence of structural brain changes that suggest a neuroanatomical phenotype, our data do not provide conclusive evidence regarding the irreversibility of these changes, as the longest follow-up was 6 months. Exploration of this question awaits further studies assessing patients longitudinally over years rather than months.

6. Conclusion

Quantitatively and longitudinally analyzed brain macrostructural changes provide new insights into radiation-induced brain impairments in NPC patients early after RT. Reduced total gray matter, and bilateral temporal lobe volumes as well as dilation of the ventricles may serve as potential biomarkers of RT-induced brain impairments and provide valuable targets for further brain recovery treatment. The observed dose-dependent alteration in bilateral temporal lobe volume indicates that a reduced irradiation dose is important for this vulnerable region.

Conflicts of interest

None.

Acknowledgment

This work was supported by the grants from the Natural Scientific Foundation of China (grant numbers: 81401399, 81201084, and 81560283), Fundamental Research Funds for the Central Universities (15ykpy35), Natural Scientific Foundation of Jiangxi Province, China (grant number: 20151BAB205049, 20142BAB205050), Medical Scientific Research Foundation of Guangdong Province (grant number: B2014162), Science and Technology Planning Project of Guangdong Province (grant number: 2012B031800102). We thank LetPub (www.letpub.com) for its linguistic assistance during the preparation of this manuscript.

Appendix A. Supplementary data

Supplementary data to this article can be found online at https://doi.org/10.1016/j.nicl.2018.04.019.

References

Bates, D., et al., 2014. Fitting Linear Mixed-effects Models Using lme4. arXiv preprint arXiv. (1406.5823).
Balentova, S., Adamkov, M., 2015. Molecular, cellular and functional effects of radiation-induced brain injury: a review. Int. J. Mol. Sci. 16 (11), 27796–27815.
Belka, C., et al., 2001. Radiation induced CNS toxicity–molecular and cellular mechanisms. Br. J. Cancer 85 (9), 1233–1239.
Buckner, R.L., et al., 2004. A unified approach for morphometric and functional data analysis in young, old, and demented adults using automated atlas-based head size normalization: reliability and validation against manual measurement of total intracranial volume. NeuroImage 23 (2), 724–738.
Cao, S.M., Simons, M.J., Qian, C.N., 2011. The prevalence and prevention of nasopharyngeal carcinoma in China. Chin. J. Cancer 30 (2), 114–119.
Chan, A.T., 2010. Nasopharyngeal carcinoma. Ann. Oncol. 21 (Suppl. 7) (vii308-12).
Chapman, C.H., et al., 2016. Diffusion tensor imaging predicts cognitive function change following partial brain radiotherapy for low-grade and benign tumors. Radiother. Oncol. 120 (2), 234–240.
Chen, J., et al., 2011. Radiation induced temporal lobe necrosis in patients with nasopharyngeal carcinoma: a review of new avenues in its management. Radiat. Oncol. 6, 128.
Cnaan, A., Laird, N.M., Slasor, P., 1997. Using the general linear mixed model to analyse unbalanced repeated measures and longitudinal data. Stat. Med. 16 (20), 2349–2380.
Connor, M., et al., 2016. Dose-dependent white matter damage after brain radiotherapy. Radiother. Oncol. 121 (2), 209–216.
Calvo, W., et al., 1988. Time- and dose-related changes in the white matter of the rat brain after single doses of X rays. Br. J. Radiol. 61 (731), 1043–1052.
Desai, S.S., et al., 2006. Radiation-induced moyamoya syndrome. Int. J. Radiat. Oncol. Biol. Phys. 65 (4), 1222–1227.
Desikan, R.S., et al., 2006. An automated labeling system for subdividing the human cerebral cortex on MRI scans into gyral based regions of interest. NeuroImage 31 (3), 968–980.
Edelstein, K., Richard, N.M., Bernstein, L.J., 2017. Neurocognitive impact of cranial radiation in adults with cancer: an update of recent findings. Curr. Opin. Support. Palliat. Care 11 (1), 32–37.
Finet, P., et al., 2010. Delayed compressive angiomatous degeneration in a case of mesial temporal lobe epilepsy treated by gamma knife radiosurgery: case report. Neurosurgery 67 (1), E218–E220.
Gazdzinski, L.M., et al., 2012. Radiation-induced alterations in mouse brain development characterized by magnetic resonance imaging. Int. J. Radiat. Oncol. Biol. Phys. 84 (5), e631–8.
Greene-Schloesser, D., Robbins, M.E., 2012. Radiation-induced cognitive impairment–from bench to bedside. Neuro-Oncology 14 (Suppl. 4), iv37–44.
Greene-Schloesser, D., et al., 2012. Radiation-induced brain injury: a review. Front. Oncol. 2, 73.
Hsiao, K.Y., et al., 2010. Cognitive function before and after intensity-modulated radiation therapy in patients with nasopharyngeal carcinoma: a prospective study. Int. J. Radiat. Oncol. Biol. Phys. 77 (3), 722–726.
Jack Jr., C.R., et al., 1989. Anterior temporal lobes and hippocampal formations: normative volumetric measurements from MR images in young adults. Radiology 172 (2), 549–554.
Karunamuni, R., et al., 2016. Dose-dependent cortical thinning after partial brain irradiation in high-grade glioma. Int. J. Radiat. Oncol. Biol. Phys. 94 (2), 297–304.
Kiang, A., et al., 2016. Long-term disease-specific and cognitive quality of life after intensity-modulated radiation therapy: a cross-sectional survey of nasopharyngeal carcinoma survivors. Radiat. Oncol. 11 (1), 127.
Kim, J.H., Jenrow, K.A., Brown, S.L., 2014. Mechanisms of radiation-induced normal tissue toxicity and implications for future clinical trials. Radiat. Oncol. J. 32 (3), 103–115.
Lin, J., et al., 2017. Radiation-induced abnormal cortical thickness in patients with nasopharyngeal carcinoma after radiotherapy. NeuroImage: Clinical 14, 610–621.
Lawrence, Y.R., et al., 2010. Radiation dose–volume effects in the brain. Int. J. Radiat. Oncol. Biol. Phys. 76 (3), S20–S27.
Long, J.D., 2011. Longitudinal Data Analysis for the Behavioral Sciences Using R. Sage.
Lv, X.F., et al., 2014. Radiation-induced changes in normal-appearing gray matter in patients with nasopharyngeal carcinoma: a magnetic resonance imaging voxel-based morphometry study. Neuroradiology 56 (5), 423–430.
Makale, M.T., et al., 2017. Mechanisms of radiotherapy-associated cognitive disability in patients with brain tumours. Nat. Rev. Neurol. 13 (1), 52–64.
Mizumatsu, S., et al., 2003. Extreme sensitivity of adult neurogenesis to low doses of X-irradiation. Cancer Res. 63 (14), 4021–4027.
Monje, M.L., et al., 2007. Impaired human hippocampal neurogenesis after treatment for central nervous system malignancies. Ann. Neurol. 62 (5), 515–520.
Morrell, C.H., Brant, L.J., Ferrucci, L., 2009. Model Choice Can Obscure Results in Longitudinal Studies. J. Gerontol. A Biol. Sci. Med. Sci. 64 (2), 215–222.
Ng, K.K., et al., 2016. Reduced functional segregation between the default mode network and the executive control network in healthy older adults: a longitudinal study. NeuroImage 133, 321–330.
Omuro, A.M., et al., 2005. Delayed neurotoxicity in primary central nervous system lymphoma. Arch. Neurol. 62 (10), 1595–1600.
Panagiotakos, G., et al., 2007. Long-term impact of radiation on the stem cell and oligodendrocyte precursors in the brain. PLoS One 2 (7), e588.
Petr, J., et al., 2016. Early and late effects of radiochemotherapy on cerebral blood flow in glioblastoma patients measured with non-invasive perfusion MRI. Radiother. Oncol. 118 (1), 24–28.
Pellmar, T.C., Schauer, D.A., Zeman, G.H., 1990. Time- and dose-dependent changes in neuronal activity produced by X radiation in brain slices. Radiat. Res. 122 (2), 209–214.
Palm, W.M., et al., 2009. Ventricular dilation: association with gait and cognition. Ann. Neurol. 66 (4), 485–493.
Prust, M.J., et al., 2015. Standard chemoradiation for glioblastoma results in progressive brain volume loss. Neurology 85 (8), 683–691.
Qiu, Y., et al., 2017. Network-level dysconnectivity in patients with nasopharyngeal carcinoma (NPC) early post-radiotherapy: longitudinal resting state fMRI study. Brain Imaging Behav. http://dx.doi.org/10.1007/s11682-017-9801-0. [Epub ahead of print].
Reuter, M., et al., 2012. Within-subject template estimation for unbiased longitudinal image analysis. NeuroImage 61 (4), 1402–1418.
Schaie, K.W., 2005. What can we learn from longitudinal studies of adult development? Res. Hum. Dev. 2 (3), 133–158.
Seibert, T.M., et al., 2017. Radiation dose-dependent hippocampal atrophy detected with longitudinal volumetric magnetic resonance imaging. Int. J. Radiat. Oncol. Biol. Phys. 97 (2), 263–269.
Simo, M., et al., 2016. Longitudinal brain changes associated with prophylactic cranial irradiation in lung cancer. J. Thorac. Oncol. 11 (4), 475–486.
Stylopoulos, L.A., et al., 1988. Longitudinal CT study of parenchymal brain changes in glioma survivors. AJNR Am. J. Neuroradiol. 9 (3), 517–522.
Tang, Y., et al., 2012. Psychological disorders, cognitive dysfunction and quality of life in nasopharyngeal carcinoma patients with radiation-induced brain injury. PLoS One 7 (6), e36529.
Team, R.C., 2014. R: A language and Environment for Statistical Computing. R Foundation for Statistical Computing. Vol. 2013 (Vienna, Austria).
Tofilon, P.J., Fike, J.R., 2000. The radioresponse of the central nervous system: a dynamic

process. Radiat. Res. 153 (4), 357–370.
Wang, S., et al., 2009. Longitudinal diffusion tensor magnetic resonance imaging study of radiation-induced white matter damage in a rat model. Cancer Res. 69 (3), 1190–1198.
Wang, H.Z., et al., 2012. Diffusion tensor imaging and 1H-MRS study on radiation-induced brain injury after nasopharyngeal carcinoma radiotherapy. Clin. Radiol. 67 (4), 340–345.
Wang, D., et al., 2016. Diffusion kurtosis imaging study on temporal lobe after nasopharyngeal carcinoma radiotherapy. Brain Res. 1648 (Pt A), 387–393.
Wei, W.I., Kwong, D.L., 2010. Current management strategy of nasopharyngeal carcinoma. Clin. Exp. Otorhinolaryngol. 3 (1), 1–12.
Xiong, W.F., et al., 2013. 1H-MR spectroscopy and diffusion tensor imaging of normal-appearing temporal white matter in patients with nasopharyngeal carcinoma after irradiation: initial experience. J. Magn. Reson. Imaging 37 (1), 101–108.
Xu, C., et al., 2017. Chemoradiotherapy versus radiotherapy alone in stage II nasopharyngeal carcinoma: a systemic review and meta-analysis of 2138 patients. J. Cancer 8 (2), 287–297.
Zhang, L.Y., Yang, H.Y., Tian, Y., 2015. Radiation-induced Cognitive Impairment. Therapeutic Targets for Neurological Diseases. 2. pp. e837.